260 Macromol. Symp. **2007**, 247, 260–270 DOI: 10.1002/masy.200750130

Morphology of Compatibilized Ternary Blends

*Cássia Alves de Freitas, Ticiane Sanches Valera, Adriana Martinelli Catelli de Souza, Nicole Raymonde Demarquette**

Summary: In this work, the evolution of the morphology of polypropylene/polystyrene/poly(methyl metacrylate) (PP/PS/PMMA) blends to which graft copolymers polypropylene-*graft*-polystyrene (PP-*g*-PS) of 2 compositions (55/45 and 70/30), polypropylene-*graft*-poly(methyl metacrylate) (PP-*g*-PMMA), or styrene-*block*-(ethylene-*co*-butadiene)-*block*-styrene (SEBS) was added has been studied. The ternary blends morphologies were predicted using phenomenological models that predict the morphology of ternary blends as a function of the interfacial tension between the blend components (spreading coefficient and free energy minimization). All blends studied presented a core-shell morphology with PS as shell and PMMA as core. The addition of PP-*g*-PS or SEBS resulted in a reduction of the size of the PS shell phase and, the addition of PP-*g*-PMMA did not seem to have any effect on the diameter of PMMA. The difference observed between the different morphologies relied on the number of droplets of core within the shell. All the phenomenological models predictions corroborated the experimental results, except when PP-*g*-PMMA was added to the blend.

Keywords: compatibilization; interfacial tension; morphology; ternary blends

Introduction

The study and development of blends formed by three or more components has raised the attention of both industrial and academic world as it can be an alternative for thermoplastic recycling.[1–15] As for any other blend, the properties of these ternary or quaternary blends are controlled by their morphology, which in this case can be predicted through the knowledge of interfacial tension between the components of the blends and some rheological properties of the individual components of the blend.[1–3,6–15] In particular 2 phenomenological models can be used to predict the morphology of a ternary or quaternary blend: spreading coefficient[6] and minimum free energy.[1,2] Table 1 presents a summary of the equations that can be used to predict the morphologies of ternary or quaternary blends and their respective criteria.

Recently, Valera et al. [16] conducted an extensive study of the morphology of PMMA/PP/PS ternary blends. The present work is an extension of the one of Valera et al.[16] In particular, the influence of addition of several compatibilizers, PP-*g*-PS (55/45), PP-*g*-PS (70/30), PP-*g*-PMMA (50/50) and SEBS on the morphology of PP/PS/PMMA ternary blends was studied. Many studies on morphologies of ternary and quaternary blends have been conducted but a few dealt with compatibilized blends.[17,18] In those few studies the authors evaluated the effect of addition of compatibilizer on the morphology both qualitatively and quantitatively. However, when doing so, they used interfacial data from the literature, consequently obtained with other polymers or calculated values obtained using harmonic or geometric means.[17] It

---

Metallurgical and Materials Engineering Department – Polytechnic School – University of São Paulo, Av. Prof. Mello Moraes, 2463, CEP:05508-900, Cidade Universitária, São Paulo, SP, Brazil
E-mail: nick@usp.br

Table 1.
Summary of the phenomenological models.

Phenomenological model	Equations
Spreading Coefficient[6]	$\lambda_{CB} = \gamma_{BA} - \gamma_{CA} - \gamma_{BC}$ (1) where, $\boldsymbol{\lambda_{ij}}$ is the spreading coefficient of ***i*** over ***j***; $\boldsymbol{\gamma_{ij}}$ is the interfacial tension between ***i*** and ***j***. **Criteria** Supposing A matrix and B and C dispersed phases. - If $\lambda_{AB} > 0$ or $\lambda_{AC} > 0$ and $\lambda_{BC} < 0$ and $\lambda_{CB} < 0$, B and C are separated phases. - If $\lambda_{BC} > 0$ and $\lambda_{CB} < 0$, C is encapsulated by B. - If $\lambda_{BC} < 0$ and $\lambda_{CB} > 0$, B is encapsulated by C. - If $\lambda_{AB} < 0$ or $\lambda_{AC} < 0$ and $\lambda_{BC} < 0$ and $\lambda_{CB} < 0$ Partial encapsulation between B and C.
Minimum Free Energy[1,2]	$(\sum A_i\gamma_{ij})_{B+C} = (4\pi)^{1/3}[n_B^{1/3}x^{2/3}\gamma_{AB} + n_C^{1/3}\gamma_{AC}](3V_C)^{2/3}$ (2) $(\sum A_i\gamma_{ij})_{B/C} = (4\pi)^{1/3}[n_B^{1/3}(1+x)^{2/3}\gamma_{AB} + n_C^{1/3}\gamma_{BC}](3V_C)^{2/3}$ (3) $(\sum A_i\gamma_{ij})_{C/B} = (4\pi)^{1/3}[n_B^{1/3}x^{2/3}\gamma_{BC} + n_C^{1/3}(1+x)^{2/3}\gamma_{AC}](3V_C)^{2/3}$ (4) where, $\mathbf{x = V_b/V_c}$, $\mathbf{V_i}$ is the volume fraction of phase ***i***; $\mathbf{n_B}$ and $\mathbf{n_C}$ are the particles numbers of B and C phases. **Criteria** The lowest value of $(\sum \mathbf{A_i}\ \boldsymbol{\gamma_{ij}})$ corresponds to the most stable morphology.

is, however, well-known that the value of interfacial tension can be altered by presence of small additives.[19] In this work, the interfacial tension between PP and PS and the influence of addition of PP-*g*-PS (55/45 and 70/30) on the interfacial tension between those two polymers was evaluated experimentally. The interfacial tension between PS and PMMA, PP and PMMA as well as the influence of addition of PP-*g*-PMMA (50/50) on the interfacial tension between those two polymers were taken from works from this research group.[20,21]

Experimental Part

Materials

In this work, three different commercial polymers were used: PP (HY6100 from Polibrasil), PS (N1841 from Innova), PMMA (DHAF from Metacril). Graft copolymers PP-*g*-PS (55/45 and 70/30) (P1045H1, P1085H1 from Basell, respectively) and PP-*g*-PMMA (P1095H1 from Basell) and SEBS (Kraton G1652 from Shell Chemical Company) were used as compatibilizers.

Blends Preparation

Two types of blends were studied in this work: binary and ternary blends. The binary blends were obtained to evaluate the interfacial tension between their components using rheological measurements following the analysis of Jacobs et al.[22] or Graebling et al.[23] The ternary blends were obtained for morphological evolution studies.

Binary Blends

Binary PP/PS blends compatibilized or not with PP-*g*-PS (55/45 and 70/30) or SEBS were obtained by mixing the blend components in an internal mixer of a torque rheometer Haake, at a temperature of 200 °C, rotor speed of 30 rpm corresponding to a shear rate of around $35 s^{-1}$,[24,25] for 7 min. After processing all binary blends were quenched in cold water. Samples for rheological and morphological analysis were obtained by compression molding. Discs of 25mm diameter_and 1.5mm thickness were molded at a temperature of 200 °C, under isotatic pressure of 18 MPa for 7 minutes.

Ternary Blends

Ternary blends were obtained by mixing the blend components in an internal mixer of a torque rheometer Haake, at a temperature of 200 °C, rotor speed of 30 rpm corresponding to a shear rate of around 35s^{-1}.[24,25]

PP/(PS + PP-g-PS or SEBS)/PMMA

In a first step, PS with or without one of the three compatibilizers (PP-g-PS 55/45 or 70/30, or SEBS) was mixed for 5 minutes. PP was then added to the blend which was mixed for 5 minutes to ensure a droplet dispersion type morphology. PMMA was then added to the PP/PS blend with or without compatibilizer. Samples of the ternary blends were then removed from the mixer chamber as a function of time (1, 2, 3, 6 and 10 minutes).

PP/PS/(PMMA or PMMA + PP-g-PMMA)

In a first step, PS was mixed for 5 minutes. PP was then added and the resulting blend mixed for 5 minutes to ensure a droplet dispersion type morphology. PMMA with or without PP-*g*-PMMA was then added to the PP/PS blend. Samples of the ternary blends were then removed from the mixer chamber as a function of time (1, 2, 3, 6 and 10 minutes).

After processing all ternary blends were quenched in cold water to fix the morphology. The morphology was then studied by scanning electron microscopy. Figure 1 shows schematically the experimental procedure used to prepare the different samples studied. Table 2 shows the binary and ternary blends volumetric fractions of the blends studied in this work.

Morphology

The binary and ternary blends morphologies were characterized by scanning electron microscopy, Philips, model XL 30, 15 kV. After cryogenical fractures, the samples were covered with gold using a Balzers sputter coater (model SCD-050). In order to obtain a good contrast between the phases in ternary blends, dissolution of PMMA was carried out using acetic acid. Quantitative analysis of the morphology was performed using Carl Zeiss Vision KS-300 software. In the quantitative analysis of the binary blends morphology, necessary to evaluate interfacial tension using rheological measurements, Saltikov's correction [26] was used.

Rheological Characterization

Experimental procedures

Rheological tests, necessary for the evaluation of interfacial tension, were carried out using a stress controlled rheometer Rheometric Scientific SR-5000 under dry nitrogen atmosphere. A parallel-plate configuration was used with a gap size of 0.7 mm and a plate diameter of 25 mm at a temperature of 200 °C. Stress sweep tests were performed to ensure that all the measurements were performed in the linear viscoelastic regime. Small amplitude oscillatory shear tests were performed for the binary blends and pure components. The zero shear viscosities of the polymers necessary to infer the interfacial tension from rheological measurements were inferred using Carreau's equation.[27] The relaxation spectra of the pure components and the blends were calculated using a nonlinear regression method available in the stress controlled rheometer SR-5000 software package from Rheometric Scientific.

Interfacial Tension Evaluation

The interfacial tension was evaluated following Jacobs et al.[22] analysis, who rewrote Palierne's generalized model[28,29] for the case of compatibilized blends. According to Jacobs et al.[22] the relaxation spectrum of a blend shows four relaxation times: two corresponding to the relaxation of the blend phases, one corresponding to

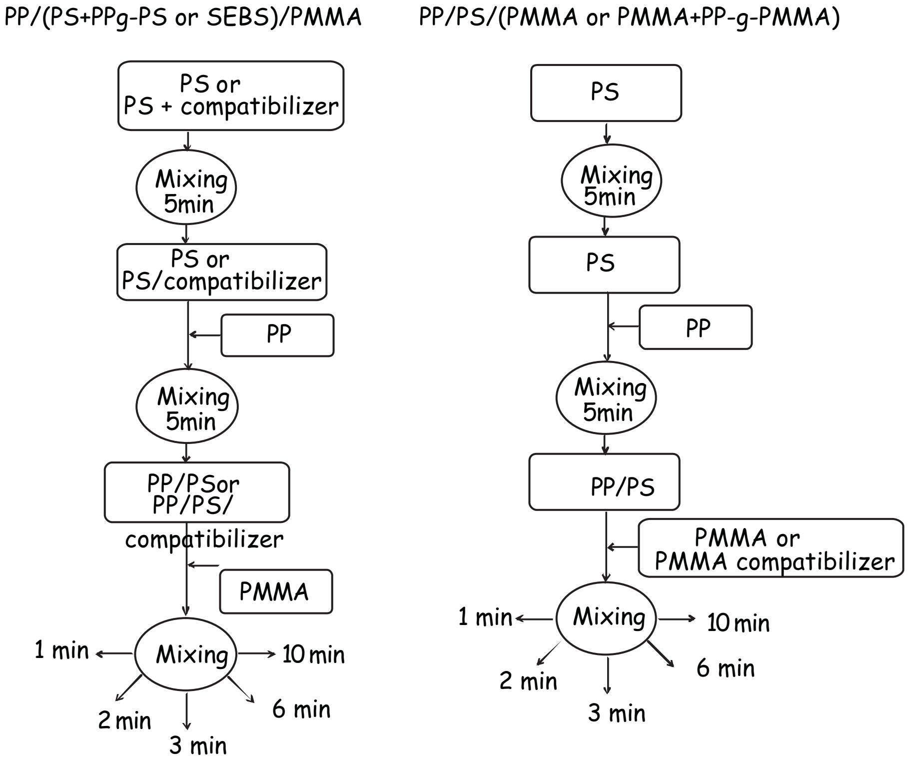

Figure 1.
Schematic representation of the experimental procedure used for the study of the evolution of morphology. Compatibilizer = SEBS or PP-*g*-PS or PP-*g*-PMMA.

the relaxation of the shape of the dispersed phase (λ_f) and a fourth one which can be attributed to the relaxation of Marangoni stresses tangential to the interface between the dispersed and matrix phase once the blend is compatibilized (λ_β).[30–37] The expressions obtained by Jacobs et al.[22] for λ_f and λ_β can be written as follows:

$$\lambda_F = \frac{\lambda_{12}}{2}\left[1 - \left(1 - 4\frac{\lambda_{11}}{\lambda_{12}}\right)^{0,5}\right] \qquad (5)$$

Table 2.
Binary and ternary blends volumetric fraction concentrations.

BLENDS		PP	PS	PMMA	PP-*g*-PS (55/45)	PP-*g*-PS (70/30)	SEBS	PP-*g*-PMMA (50/50)
Binary	**PP/PS**	80	20	–	–	–	–	–
	PP/PS + PP-*g*-PS(55/45)	80	18	–	2	–	–	–
	PP/PS + PP-*g*-PS(70/30)	80	18	–	–	2	–	–
	PP/PS + SEBS	80	18	–	–	–	2	–
	PP/PMMA + PP-*g*-PMMA(50/50)	80	–	18	–	–	–	2
Ternary	**PP/PS/PMMA**	80	15	5	–	–	–	–
	PP/PS + PP-*g*-PS(55/45)/PMMA	80	13.5	5	1.5	–	–	–
	PP/PS + PP-*g*-PS(70/30)/PMMA	80	13.5	5	–	1.5	–	–
	PP/PS + SEBS/PMMA	80	13.5	5	–	–	1.5	–
	PP/PS/PMMA + PP-*g*-PMMA(50/50)	80	15	4.5	–	–	–	0.5

and

$$\lambda_\beta = \frac{\lambda_{12}}{2}\left[1 + \left(1 - 4\frac{\lambda_{11}}{\lambda_{12}}\right)^{0,5}\right] \tag{6}$$

with

$$\lambda_{11} = \frac{R_V \eta_m}{4\gamma} \frac{(19K+16)[2K+3-2\phi(K-1)]}{10(K+1) + \frac{\beta_{20}}{\gamma}(13K+12) - 2\phi\left((5K+2) + \frac{\beta_{20}}{2\gamma}(13K+8)\right)} \tag{7}$$

$$\lambda_{12} = \frac{R_V \eta_m}{8\beta_{20}} \frac{10(K+1) + \frac{\beta_{20}}{\gamma}(13K+12) - 2\phi\left((5K+2) + \frac{\beta_{20}}{2\gamma}(13K+8)\right)}{(1-\phi)} \tag{8}$$

where: R_v is volume average radius, η_m is the viscosity of the matrix, ϕ is volume fraction of dispersed phase, K is viscosity ratio, γ is interfacial tension and β_{20} is the interfacial modulus.

For the limiting case $\beta_{20} = 0$, the relaxation of the shape of the dispersed phase (λ_f) coincides with the relaxation of the shape of the dispersed phase for the simplified Palierne model[23]:

$$\lambda_F = \frac{R_V \eta_m}{4\gamma} \times \frac{(19K+16)[2K+3-2\phi(K-1)]}{10(K+1) - 2\phi(5K+2)} \tag{9}$$

where every symbol has been defined above.

Recently, Wang and Velankar[38] corrected and rewrote those equations as they had been published with a typographical error in the original paper of Jacobs et al.[22] The equations reported by Wang and Velankar[38] appeared in a slightly different algebraic form than in the original paper of Jacobs et al.[22] to remain finite in the case $\beta_{20} = 0$ but are equivalent to equations (5)–(8) presented here.

Analysing the relaxation spectrum of binary blends, it is therefore possible, if four relaxation times are identified to solve equations (5) and (6) to infer the interfacial tension between the components of the blends. In the case of uncompatibilized blends, only three relaxation times are observed, two corresponding to the isolated phases of the blend and λ_f. In this case, the equation (9) can be used to infer interfacial tension.

Results and Discussion

Interfacial tension evaluation

Figure 2 presents the typical relaxation spectra of PP and PS pure phases, PP/PS blend compatibilized or not with PP-*g*-PS (55/45 and 70/30) and SEBS.

It can be seen that PP/PS uncompatibilized blend and PP/PS blends compatibilized with PP-*g*-PS (55/45 and 70/30) present only two relaxation times: one corresponding to the superposition of relaxation of two phases of the blend and a second one which corresponds to the relaxation of the shape of the dispersed phase (λ_f). In the case of PP/PS blend compatibilized with SEBS three relaxation times can be observed: one related to the superposition of relaxation of two phases of the blend, one which corresponds to the relaxation of the shape of the dispersed phase (λ_f) and one which corresponds to the relaxation of Marangoni stresses arouse from the presence of SEBS (λ_β).

In this work, the interfacial tension between PP and PS to which SEBS had been added was evaluated following the procedures of Jacobs et al. [22] Due to the low compatibilizer concentrations used to modify the PP/PS blends and due the fact that only 2 relaxation times were observed on relaxation spectra of PP/PS blends compatibilized with PP-*g*-PS (55/45 and 70/30), it was assumed that simplified

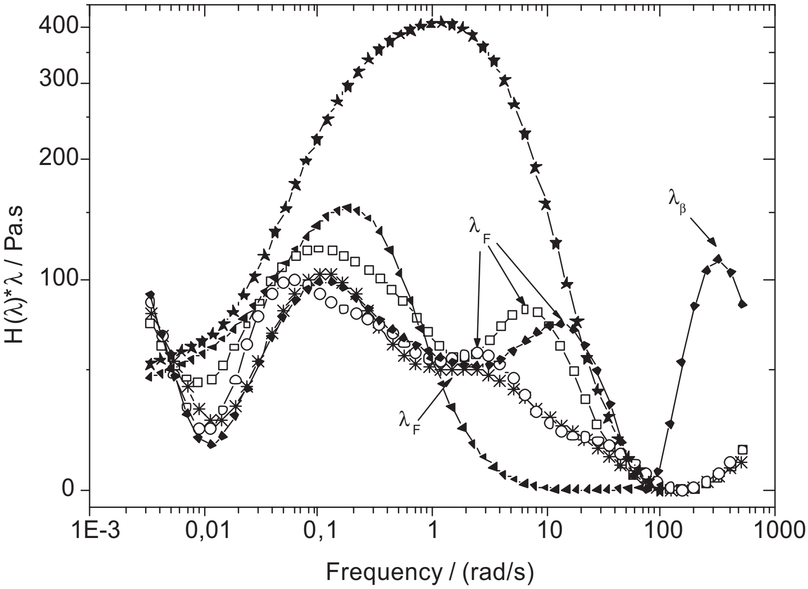

Figure 2.
Relaxation spectrum for the pure phases (★) PP, (◀) PS and blends (□) PP/PS, (✳) PP/PS + PP-*g*-PS (55/45), (○) PP/PS + PP-*g*-PS (70/30) and (◆) PP/PS + SEBS.

Palierne emulsion model could be used to evaluate the interfacial tension between PP and PS to which PP-*g*-PS (55/45 and 70/30) had been added. The contribution of the dispersed phase was then considered as a sum of the contribution of the dispersed phase (PS) and the contribution of the compatibilizer (PP-*g*-PS (55/45 and 70/30)).

Table 3 summarizes the average values of the relaxation times of the PP/PS blends studied here as well as the data necessary for the evaluation of interfacial tension (R_v, η_d and K). The interfacial tension between PMMA and PS, PP and PMMA as well as the influence of addition of PP-*g*-PMMA (50/50) on the interfacial tension between those two polymers taken from works of this research group [20,21] are also reported in Table 3.

Experimental morphologies

In order to study the morphology evolution of the ternary blends studied in this work the morphologies of several samples of PP/PS/PMMA blends, compatibilized or not, were observed. The samples were obtained according to the procedures summarized in Figure 1. Figures 3 and 4 show the morphology evolution of PP/PS/PMMA + PP-*g*-PMMA and PP/PS + PP-*g*-PS (70/30)/PMMA (similar behavior was obtained for PP/PS/PMMA and PP/PS + PP-*g*-PS

Table 3.
Interfacial Tension obtained by Relaxation Spectrum analysis.

BLEND	R_v (μm)	η_d (Pa.s)	K	λ_f (s)	λ_β (s)	γ (mN/m)	β_{20}(N/m)
PP/PS	2.98	2400	0.343	5.8	–	6.7	–
PP/PS + PP-*g*-PS (55/45)	0.93	3000	0.429	3.3	–	3.9	–
PP/PS + PP-*g*-PS (70/30)	1.12	3500	0.500	3.3	–	3.5	–
PP/PS + SEBS	1.24	3600	0.514	6.2	288.6	2.9	0.4×10^{-5}
PMMA/PP[21]						7.1	
PMMA/PS[21]						1.7	
PP/PMMA + PP-*g*-PMMA (50/50)[20]						4.6	

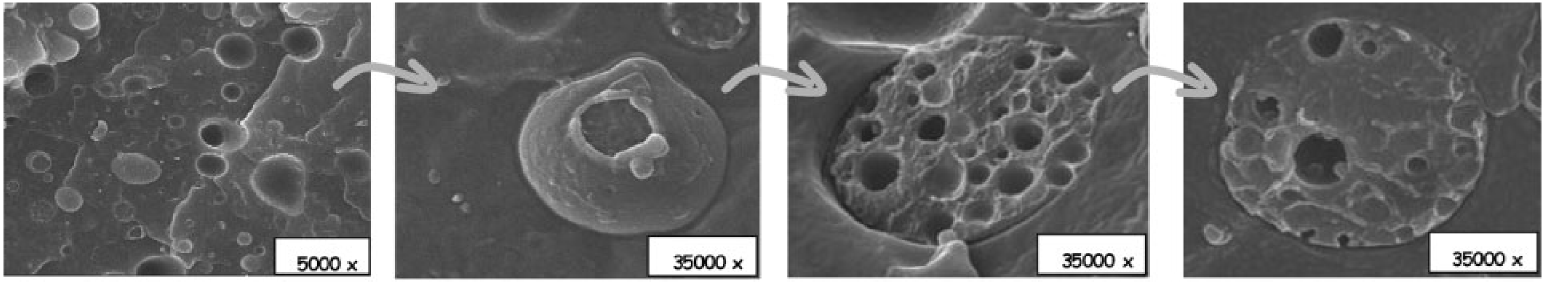

PP/PS (5min) a)

PP/PS/PMMA (+1min) b)

PP/PS/PMMA (+6min) c)

PP/PS/PMMA (+10 min) d)

Figure 3.
Evolution of the morphology of PP/PS/PMMA + PP-*g*-PMMA as a function of time after solvent etching using acetic acid.

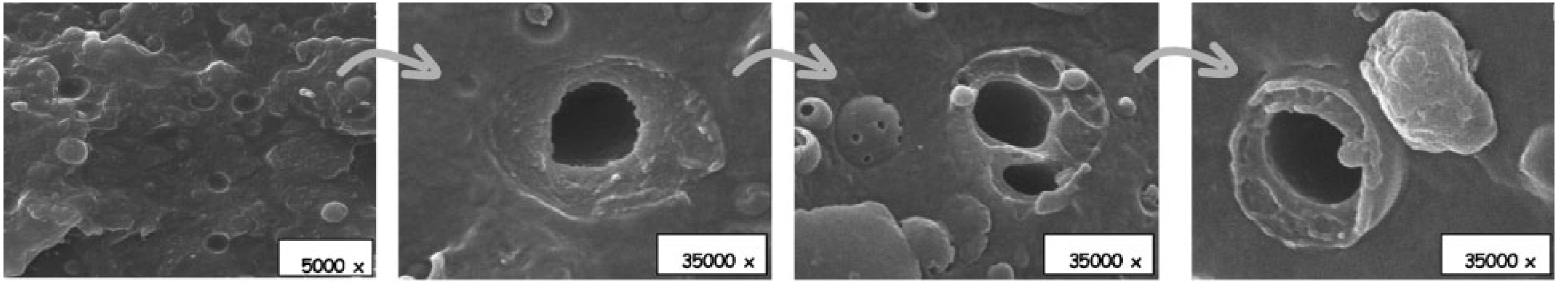

PP/PS (5min) a)

PP/PS/PMMA (+1min) b)

PP/PS/PMMA (+6min) c)

PP/PS/PMMA (+10 min) d)

Figure 4.
Evolution of the morphology of PP/PS + PP-*g*-PS (70/30)/PMMA as a function of time after solvent etching using acetic acid.

(55/45)/PMMA, and PP/PS + SEBS/PMMA, respectively) ternary blends. Figures 3a and 4a show the dispersed phase morphology of PP/PS with or without compatibilizer blends before the PMMA addition. Figure 3b and 4b present the morphology evolution once the PMMA has been added to the binary PP/PS blend. It can be seen from Figures 3b and 4b that when PMMA was added to the PP/PS blend it tended to penetrate the PS droplets forming a core-shell morphology with only one PMMA drop inside the PS shell. Subsequently, the core droplet of PMMA deformed and broke up into smaller droplets (Figures 3c and 4c). The difference observed in the final morphologies (Figures 3d and 4d) relied on the number of PMMA core particles present in the PS shell: it reduced to one when SEBS and PP-*g*-PS (70/30) was used. These qualitative morphological observations indicated that the addition of compatibilizer have an effect on the type of blend morphology.

Table 4 shows a schematic representation of equilibrium morphologies obtained and quantitative results of the ternary blends morphology studied in this work. It can be seen that upon the addition of PP-*g*-PS or SEBS the core-shell diameter of the composite droplets decreases. This behavior is expected as PP-*g*-PS and SEBS act as compatibilizers for PP/PS binary blends. The addition of PP-*g*-PMMA does not seem to have any effect on the diameter of PMMA. This can be easily understood if we remember that PMMA is thermodynamically driven to be in contact with PS and not PP. However, when PP-*g*-PMMA was added to the PP/PS blend some PMMA migrated from the core of the PS droplet (see Figure 3d) to the interface between PS and PP as can be seen in Figure 5 which shows the detailed morphology of PP/PS/PMMA + PP-*g*-PMMA (50/50). This can be explained by the decrease of interfacial tension between PP and PMMA involved by the addition of PP-*g*-PMMA; the interfacial tension reduced from 7.1 to 4.6 mN/m.[20,21]

The core-shell morphologies presented in Figures 3 and 4 differ with respect to the number of core particles inside the shell phase. These results could not be explained in light of change of interfacial tension between PS and PMMA which is not affected by the addition of the compatibilizers used in this work. However, the results reported seem to indicate that the number of core particles (PMMA) is inversely proportional to the viscosity of the shell (PS + compatibilizer) (see values presented in Table 5). This is not expected

Table 4.
Schematic representation of equilibrium morphologies obtained and quantitative results of the ternary blends morphology (d_v). (grey = PMMA or PMMA + PP-*g*-PMMA and black = PS or (PS + PP-*g*-PS or SEBS)).
PP matrix

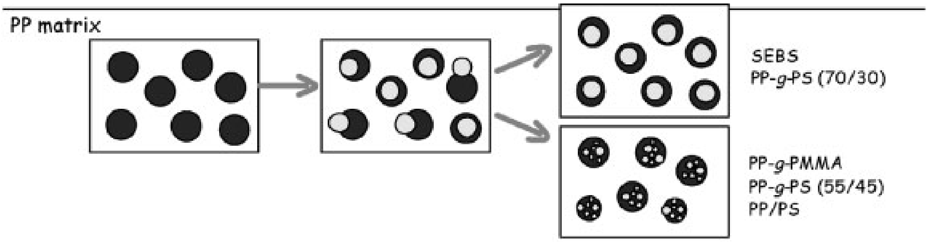

Volume average diamater, d_v (μm)

PP/PS/PMMA		PP/PS + PP-*g*-PS (70/30)/PMMA		PP/PS + PP-*g*-PS (55/45)/PMMA		PP/PS + SEBS/PMMA		PP/PS/PMMA + PP-*g*-PMMA (50/50)	
PS	PMMA	PS	PMMA	PS	PMMA	PS	PMMA	PS	PMMA
2.8	0.4	1.0	0.6	2.0	0.8	1.6	0.6	2.8	0.4

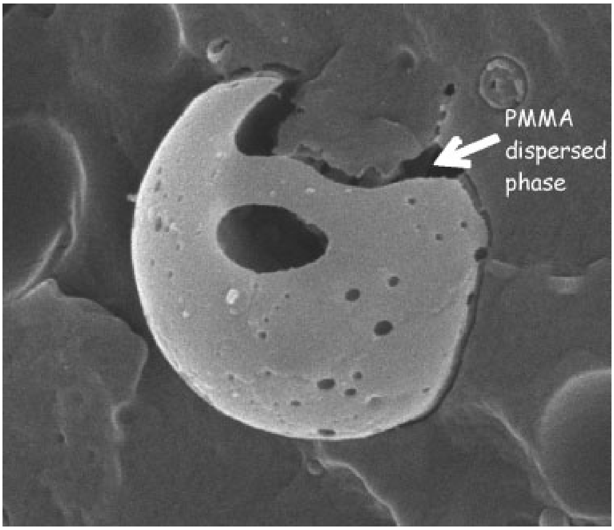

Figure 5.
Detailed morphology of PP/PS/PMMA + PP-*g*-PMMA (50/50).

as a lower viscosity ratio (originated from an increase of shell viscosity) should result in a smaller dispersed phase size. The results seem to indicate that when either SEBS or PP-*g*-PS (70/30) were added to the blend the mixing time was sufficient for break up and coalescence to occur, whereas this was not the case when no compatibilizer, PP-*g*-PS (55/45) or PP-*g*-PMMA (50/50) were added.

Table 5.
Viscosities of the dispersed phases, with or without compatibilizer, at 35^{-1}s.

Dispersed phases	Viscosity (Pa.s), 35^{-1}s
PS	940
PS + SEBS	950
PS + PP-*g*-PS (70/30)	880
PS + PP-*g*-PS (55/45)	800
PMMA + PP-*g*-PMMA (50/50)	4190
PMMA	3700

Morphology prediction

Using the interfacial tension reported in Table 3 it was possible to evaluate the spreading coefficient (equation 1) and minimum free energy (equations 2, 3 and 4). More details of the assumptions made to predict the morphologies are reported in Valera et al.[16] These values are reported in Table 6 and the predicted morphologies are reported in Table 7.

The predicted morphologies by spreading coefficient and minimum free energy models corroborate the morphologies experimentally observed for ternary blends in most of the cases, except for PP/PS/PMMA + PP-*g*-PMMA blend. The addi-

Table 6.
Values of spreading coefficient and minimum free energy.

POLYMER BLEND	Spreading Coefficient (mN/m)			Minimum Free Energy (mN/m)		
	$\lambda_{PS/PMMA}$	$\lambda_{PP/PMMA}$	$\lambda_{PMMA/PS}$	$G_{PS+PMMA}$	$G_{PS/PMMA}$	$G_{PMMA/PS}$
PP/PS/PMMA	−1.3	−12.1	−2.1	0.067	0.060	0.063
PP/PS + PP-*g*-PS (55/45)/PMMA	1.5	−9.3	−4.9	0.053	0.038	0.063
PP/PS + PP-*g*-PS (70/30)/PMMA	1.9	−8.9	−5.3	0.051	0.035	0.063
PP/PS/PMMA + PP-*g*-PMMA (50/50)	−3.8	−9.6	0.4	0.055	0.060	0.044
PP/PS + SEBS/PMMA	2.5	−8.3	−5.9	0.048	0.030	0.063

Table 7.
Predicted morphologies.

POLYMER BLEND	Spreading Coefficient	Minimum Free Energy
PP/PS/PMMA	*Partial Encapsulating*	PS engulfs PMMA
PP/PS + PP-*g*-PS (55/45)/PMMA	PS engulfs PMMA	PS engulfs PMMA
PP/PS + PP-*g*-PS (70/30)/PMMA	PS engulfs PMMA	PS engulfs PMMA
PP/PS/PMMA + PP-*g*-PMMA (50/50)	*PMMA engulf PS*	*PMMA engulf PS*
PP/PS + SEBS/PMMA	PS engulfs PMMA	PS engulfs PMMA

tion of PP-*g*-PS or SEBS compatibilizer lead to a decrease of interfacial tension between PP and PS which promoted a core-shell morphology corroborating the predictions of the phenomenological models; the addition of PP-*g*-PMMA lead to a decrease of interfacial tension between PP and PMMA components which promoted the migration of PMMA to the interface between PS and PP, however the decrease of interfacial tension was not large enough for PMMA to encapsulate PS as predicted by spreading coefficient and minimum free energy models.

Conclusions

In this work, the morphology evolution of PP/PS/PMMA ternary blends, with or without compatibilizers (PP-*g*-PS (55/45 and 70/30), SEBS and PP-*g*-PMMA), was studied. A core-shell morphology with PS as shell and PMMA as core was obtained for all the studied blends. When PMMA, compatibilized or not, was added to the binary blend of PP/PS (with or without compatibilizer), it tended to penetrate the PS droplets forming a core-shell morphology with only one drop of PMMA inside the PS shell. Subsequently, the core droplet of PMMA deformed and broke up into smaller droplets. The difference observed in the final morphologies relied on the number of PMMA core particles present in the PS shell: it reduced to one when SEBS and PP-*g*-PS (70/30) was used. The addition of PP-*g*-PS or SEBS was shown to decrease the core-shell diameter of the composite droplets. The addition of PP-*g*-PMMA did not seem to have any effect on the diameter of PMMA. Furthermore, when PP-*g*-PMMA was added to the PP/PS blend some PMMA migrated from the core of the PS droplet to the interface between PS and PP. The equilibrium morphologies were compared to the predictions of spreading coefficient and minimum free energy phenomenological models. The predicted morphologies corroborated the morphologies experimentally observed for the ternary blends studied in most of the cases.

Acknowledgements: The authors would like to thank the Polibrasil, Innova, Metacril, Shell and Basell for supplying the materials; FAPESP and CAPES for financial support.

[1] H. F. Guo, S. Packirisamy, N. V. Gvozdic, D. J. Meier, *Polymer* **1997**, *38*, 785.
[2] H. F. Guo, N. V. Gvozdic, D. J. Meier, *Polymer* **1997**, *38*, 4915.
[3] J. Reignier, B. D. Favis, *Macromolecules* **2000**, *33*, 6998.
[4] J. Reignier, B. D. Favis, M. C. Heuzey, *Polymer* **2003**, *44*, 49.
[5] J. Reignier, B. D. Favis, *Mater. Interfaces Electrochem. Phenom.* **2003**, *49*, 1014.
[6] S. Y. Hobbs, M. E. J. Dekkers, V. H. Watkins, *Polymer* **1988**, *29*, 1598.
[7] M. Lee, C. Tzoganakis, *J. M. Proceedings of the Annual Technical Conference ANTEC; Orlando, FL,* **2000**; SPE: Brookfield.
[8] E. B. Nauman, D. Q. He, *Chem. Eng. Sci.* **2001**, *56*, 1999.
[9] S. Urashita, T. Kawakatsu, M. Doi, *Prog. Theor. Phys. Suppl.* **2000**, *138*, 412.
[10] S. Horiuchi, Y. K. Matchariyakul, T. Kitano, *Macromolecules* **1997**, *30*, 3664.
[11] N. Nemirovski, A. Siegmann, M. J. Narkis, *Macromol. Sci. Phys.* **1995**, *B34*, 459.
[12] A. K. Gupta, K. R. Srinivasan, *J. Appl. Polym. Sci.* **1993**, *47*, 167.
[13] I. Lusinov, C. Pagnoulle, R. Jérôme, *Polymer* **2000**, *41*, 7099.

[14] M. Hemmati, H. Nazokdast, H. S. Panahi, *J. Appl. Polym. Sci.* **2001**, *82*, 1129.

[15] K. P. Tchomakov, B. D. Favis, *Proceedings of the Annual Technical Conference ANTEC; San Francisco, CA, 2002; SPE: Brookfield.*

[16] T. S. Valera, A. T. Morita, N. R. Demarquette, *Macromolecules* **2006**, *39*, 2663.

[17] T. S. Omonov, C. Harrats, G. Groeninckx, *Polymer* **2005**, *46*, 12322.

[18] M. A. Debolt, R. E. Robertson, *Polym. Eng. Sci.* **2006**, *46*, 385.

[19] N. R. Demarquette, M. R. Kamal, *J. Appl. Polym. Sci.* **1998**, *70*, 75.

[20] P. S. Calvão, "Dissertation", Master Thesis, University of Sao Paulo, Brazil **2004**.

[21] P. S. Calvão, M. Yee, N. R. Demarquette, *Polymer* **2005**, *46*, 2610.

[22] U. Jacobs, M. Fahrländer, J. Winterhalter, C. Friedrich, *J. Rheol.* **1999**, *43*, 1495.

[23] D. Graebling, R. Muller, J. F. Palierne, *Macromolecules*, **1993**, *26*, 320.

[24] M. Bousmina, A. Ait-Kadi, J. B. Faisant, *J. Rheol.* **1999**, *43*, 415.

[25] T. S. Valera, N. R. Demarquette, S. M. Toffoli, *J. Polym. Eng.* **2004**, *24*, 409.

[26] E. E. Underwood, *Quantitative stereology;* Addison-Wesley: Mass, **1970**.

[27] P. J. Carreau, D. Kee, R. Chhabra, *Rheology of polymeric systems principles and applications*, Carl Hanser, Munich, Germany **1997**.

[28] J. F. Palierne, *Rheologica Acta* **1990**, *29*, 204.

[29] J. F. Palierne, *Rheologica Acta* **1991**, *30*, 497.

[30] R. E. Riemann, H. J. Cantow, C. Friedrich, *Polym. Bull.* **1996**, *36*, 637.

[31] R. E. Riemann, H. J. Cantow, C. Friedrich, *Macromolecules* **1997**, *18*, 5476.

[32] M. Fahrländer, M. Bruch, T. Menke, C. Friedrich, *Rheol. Acta* **2001**, *40*, 1.

[33] E. Van Hemelrijck, P. Van Puyvelde, S. Velankar, C. W. Macosko, P. Moldenaers, *J. Rheol.* **2004**, *48*, 143.

[34] E. Van Hemelrijck, P. Van Puyvelde, S. Velankar, C. W. Macosko, P. Moldenaers, *J. Rheol.* **2005**, *49*, 783.

[35] S. Velankar, P. Van Puyvelde, J. Mewis, P. J. Moldenaers, P. J. Rheol. **2004**, *48*, 725.

[36] S. Velankar, P. Van Puyvelde, J. Mewis, P. Moldenaers, *J. Rheol.* **2001**, *45*, 1007.

[37] M. Moan, J. Huitric, P. Médéric, J. Jarrin, *J. Rheol.* **2000**, *44*, 1227.

[38] J. Wang, S. Velankar, *Rheologica Acta*, **2006**, *45*, 741.